JOURNAL OF SOLID STATE CHEMISTRY 56, 148–157 (1985)

$Ta_4P_4S_{29}$: A New Tunnel Structure with Inserted Polymeric Sulfur

M. EVAIN, M. QUEIGNEC, R. BREC, AND J. ROUXEL

Laboratoire de Chimie des Solides, L.A. 279,
2, rue de la Houssinière—44072 Nantes Cedex, France

Received May 21, 1984; in revised form July 16, 1984

$Ta_4P_4S_{29}$ was prepared from the elements heated together in stoichiometric proportions in an evacuated Pyrex tube for 10 days at 500°C. The crystal symmetry is tetragonal, space group $P4_32_12$, with the cell parameters: $a = b = 15.5711(7)$ Å, $c = 13.6516(8)$ Å, $V = 3309.9(5)$ Å^3, and $Z = 4$. The structure calculations were conducted from 2335 reflections and 146 variables, leading to $R = 0.033$. The structure basic framework, corresponding to the chemical composition $[TaPS_6]$, is made of biprismatic bicapped $[Ta_2S_{12}]$ units (average $d_{Ta-S} = 2.539$ Å), including sulfur pairs (average $d_{S-S} = 2.039$ Å), bonded to each other through $[PS_4]$ tetrahedral groups (average $d_{P-S} = 2.044$ Å) sharing sulfurs. This framework leaves large tunnels running along the c axis of the cell and in which $(S_{10})_\infty$ sulfur chains are found to be inserted (average $d_{S-S} = 2.052$ Å and S–S–S = 105.75°). Diamagnetic and semiconducting $Ta_4P_4S_{29}$ can be formulated: $Ta_4^{V}P_4^{V}(S^{-II})_{16}(S_2^{-II})_4(S_5^{0})$.

1. Introduction

It has been extensively shown that chalcogens, in their combination with phosphorus and transition metals, form mostly low-dimensional phases. The first example of such structural behavior is provided by the MPS_3 family. These phases were first synthesized by Friedel (*1*) who, as early as 1894, was able to prepare and characterize several members of the series (M = Fe, Sn, Zn, Pb, Hg) and to recognize the layer character of the compounds. Fundamental and applied interest revived after the structural work of Hahn and Klingen (*2–6*) who showed that the MPX_3 bidimensional compounds derived directly from a $CdCl_2$ or CdI_2 structural type. More recently, several new members of the M–P–S systems (M = V, Nb, and Ta) were prepared (*7–13*). With vanadium as cation, and in consonance with very covalent-type bonding, only low-dimensional compounds have been obtained to date. They are (2D) $P_{0.2}VS_2$ (*7*), (1D) PV_2S_{10} (*8*), and (2D) $V_2P_4S_{13}$ (*9*). With niobium, two-dimensional structures have been found, with (2D) PNb_2S_{10} (*10*), (2D) $P_2Nb_4S_{21}$ (*11*), and (2D) P_2NbS_8 (*12*). However, in the case of this latter material, a (3D) modification was also observed (*13*), in accord with the more ionic Nb–S bond. With more electropositive tantalum, tridimensional networks are expected to form more generally; the first Ta–P–S compound to be obtained, $TaPS_6$ (*14*), exhibits a 3D atomic arrangement. It comes as no surprise that $Ta_4P_4S_{29}$, for which the synthesis and structural determination are reported herein, is also a 3D material.

2. Experimental

$Ta_4P_4S_{29}$ can be obtained by heating stoichiometric proportions of the pure ele-

0022-4596/85 $3.00

TABLE I

ANALYTICAL AND CRYSTALLOGRAPHIC DATA. PARAMETERS OF THE X-RAY DATA COLLECTION AND REFINEMENT

1. Physical, crystallographic, and analytical data

Formula $Ta_4P_4S_{29}$ Molecular weight: 1777.54

Theoretical weight fraction concentration

P: 6.97% S: 52.31% Ta: 40.72%

Microprobe analysis:

P: 6.5(2)% S: 51.1(9)% Ta: 42(1)%

Crystal symmetry tetragonal; Space group $P4_32_12$

Cell parameters (293K):

$a = b = 15.5711(7)$ Å $c = 13.6516(8)$Å

$V = 3309.9(5)$ Å^3 $Z = 4$

Density $d_{cal} = 3.591$

Absorption factor: $\mu(\lambda MoK\alpha)$: 149.95 cm^{-1}

Crystal size: 0.3 × 0.05 × 0.05 mm^3

2. Data collection

Temperature 293 K. Radiation Mo$K\alpha$

Monochromator: oriented graphite (002). Scan mode: $\omega/2\theta$

Recording angle range: 3–30°. Scan angle 1.00 + 0.35 tan θ

Values determining the scan speed:

SIGPRE: 0.85, SIGMA: 0.03, VPRE = 5° · min^{-1}, TMAX = 180 sec

Standard reflexion: $82\bar{6}$ $9\bar{1}7$ $10\bar{4}4$. Periodicity: 3600 sec

ABSMIN: 0.4546 ABSMAX: 0.6067 ABSAVG: 0.5004

3. Refinement conditions

Reflections for the refinement of the cell dimensions: 25

Recorded reflections in the quarter-space: 10,955

Utilized reflections: 2335 with $I \geq 3\,\sigma\,(I)$

Refined parameters: 146

Reliability factors: $R = \Sigma[|F_0|-|F_c|]/\Sigma|F_0|$

$R_\omega = [\Sigma_\omega(|F_0|-|F_c|)^2/\omega F_0^2]^{1/2}$

4. Refinement results

$R = 0.033$ $R_\omega = 0.036$

Extinction coefficient: $E_c = 1.55(9) \times 10^{-8}$

Difference Fourier maximum peak intensity: 1.2(5) e^-/Å^3

ments in evacuated Pyrex tubes, at 500°C for 10 days, followed by a 10-hr cooling. Under these conditions, the bulk of the sample consists of microcristalline powder, whereas on its surface, large black needle-like crystals can be found. Their analysis was conducted with a microprobe (microsonde Ouest CNEXO), using a $TaPS_6$ single crystal as standard (Table I). Single crystal X-ray study indicated that the compound exhibits tetragonal symmetry. A superstructure has been detected, corresponding to a doubling of the c parameter. The conditions limiting possible reflexions on the (hkl) planes of the substructure, $00l$ with $l = 2n$ and $h00$ with $h = 2n$, correspond to

TABLE II

$Ta_4P_4S_{29}$ X-RAY POWDER DIFFRACTION DATA

d_{obs} (Å)	d_{calc} (Å)	hkl	100 × I/I_0[a]	d_{obs} (Å)	d_{calc} (Å)	hkl	100 × I/I_0[a]
10.99	11.01	110	28.6	2.1631	2.1628	216	19.9
7.78	7.78	200	60.7	2.1150	2.1150	702	0.7
6.95	6.96	210	0.9	2.1028	2.1031	534	12.5
5.807	5.801	112	100.0		2.1028	226	
5.497	5.505	220	7.1	2.0963	2.0957	712	3.8
5.129	5.132	202	3.8	2.0658	2.0654	316	4.3
4.928	4.924	310	53.5		2.0658	604	
4.871	4.874	212	13.6	2.0591	2.0588	642	1.2
4.283	4.285	222	20.6	2.0477	2.0478	614	1.4
4.131	4.131	302	1.9	2.0408	2.0410	722	3.1
3.990	3.993	312	4.7	2.0130	2.0130	326	1.4
3.669	3.670	330	9.3	1.9964	1.9967	624	4.0
3.413	3.413	004	2.0	1.9805	1.9805	544	2.9
3.383	3.381	402	0.3	1.9586	1.9586	732	4.0
3.302	3.304	412	4.4	1.9493	1.9489	416	10.7
3.258	3.260	114	1.2	1.9051	1.9047	426	5.8
3.234	3.232	332	0.4	1.8886	1.8883	820	1.9
3.1015	3.1016	422	20.4	1.8587	1.8584	742	5.3
3.0629	3.0645	214	10.6	1.8512	1.8503	714	2.3
2.9001	2.9007	224	0.8	1.8353	1.8351	660	3.1
2.8505	2.8516	304	3.6	1.8247	1.8248	644	4.1
2.8320	2.8333	432	6.2		1.8245	516	
2.8047	2.8050	314	8.2	1.8102	1.8101	750	1.6
2.7868	2.7875	512	5.0	1.7883	1.7881	526	3.7
2.7518	2.7526	440	5.0	1.7499	1.7496	752	7.7
2.6766	2.6777	324	5.4	1.7216	1.7215	654	1.4
2.6703	2.6704	530	3.8	1.7001	1.7006	616	1.0
2.6615	2.6624	522	9.6	1.6966	1.6963	108	2.7
2.5940	2.5952	600	8.0	1.6865	1.6869	842	3.4
2.5650	2.5663	404	1.4	1.6676	1.6675	912	1.9
2.5523	2.5528	442	18.6	1.6617	1.6614	546	3.3
2.5310	2.5321	414	3.9	1.6579	1.6574	218	1.9
2.4993	2.4993	334	17.6	1.6526	1.6523	824	1.6
2.4863	2.4869	532	1.7	1.6414	1.6413	930	3.6
2.4609	2.4620	620	17.2	1.6299	1.6299	228	1.4
2.4361	2.4373	424	2.7	1.6247	1.6248	636	1.7
2.3972	2.3969	612	0.1	1.6209	1.6211	308	3.8
2.3155	2.3160	622	5.0	1.6165	1.6163	664	2.0
2.3001	2.3004	434	10.5	1.6079	1.6076	834	11.8
2.2917	2.2908	542	5.9	1.5877	1.5871	328	2.1
2.2756	2.2757	514	3.0	1.5827	1.5823	556	1.5
2.2286	2.2282	116	0.7	1.5663	1.5663	646	1.8
2.2046	2.2062	524	4.1	1.5583	1.5584	726	2.6
2.2025	2.2021	550	3.0	1.5508	1.5511	844	1.2
2.1836	2.1839	206	0.3	1.5426	1.5432	904	2.5

Note. Intensities calculated with Lazy Pulverix program. $a = b = 15.5711(7)$ Å, $c = 13.6516(8)$ Å

[a] Calculated intensities.

TABLE III

$TaPS_6$ X-RAY POWDER DIFFRACTION DATA

d_{obs} (Å)	d_{calc} (Å)	hkl	$100 \times I/I_0$[a]	d_{obs} (Å)	d_{calc} (Å)	hkl	$100 \times I/I_0$[a]
7.928	7.938	200	100.0	2.0825	2.0822	633	4.3
6.249	6.246	211	72.0	2.0600	2.0606	604	6.9
5.668	5.670	112	94.8	2.0241	2.0244	435	14.7
5.063	5.061	202	3.3	1.9945	1.9945	624	9.1
4.173	4.175	321	27.0	1.9875	1.9871	732	2.3
3.990	3.989	312	1.6	1.9845	1.9846	800	2.0
3.697	3.695	411	7.3	1.9618	1.9616	525	4.1
3.398	3.397	402	0.7	1.9477	1.9475	741	2.3
3.253	3.251	332	3.1	1.9247	1.9253	820	4.7
3.106	3.105	323	23.7	1.9165	1.9173	406	0.1
3.0862	3.0865	431	8.8	1.8707	1.8711	660	4.5
3.0354	3.0350	204	4.1	1.8398	1.8399	831	2.7
2.8928	2.8918	413	6.7	1.8286	1.8288	644	5.7
2.8769	2.8767	521	1.5	1.8149	1.8146	217	3.4
2.8336	2.8349	224	1.3	1.8032	1.8034	545	3.8
2.8137	2.8136	512	7.7	1.7910	1.7911	516	2.7
2.8055	2.8066	440	6.2	1.7770	1.7768	752	5.9
2.6458	2.6461	600	5.9	1.7591	1.7586	635	2.1
2.5704	2.5707	433	32.0	1.7270	1.7266	327	3.1
2.5105	2.5103	620	14.5	1.6870	1.6871	417	0.7
2.4629	2.4643	215	1.0	1.6701	1.6693	851	3.6
2.4447	2.4457	523	15.0	1.6610	1.6610	824	3.0
2.4364	2.4365	541	6.7	1.6427	1.6423	008	5.7
2.4108	2.4110	424	8.2	1.6252	1.6258	664	1.0
2.2561	2.2564	325	12.5	1.6158	1.6157	437	1.6
2.2427	2.2421	613	1.6	1.6078	1.6082	208	3.2
2.1706	2.1705	415	1.8	1.6009	1.6000	941	4.3
2.1572	2.1577	543	4.2	1.5873	1.5877	860	3.4
2.1489	2.1492	116	10.0	1.5682	1.5676	716	9.3
2.1247	2.1246	552	7.2	1.5614	1.5616	844	4.5

[a] Intensities calculated with Lazy Pulverix program. $a = b = 15.8768(9)$ Å, $c = 13.138(1)$ Å.

$P4_22_12$ space group, whereas, with the superstructure, the reflection conditions ($00l$, $l = 4n$ and $h00$, $h = 2n$) correspond to the space groups $P4_12_12$ and $P4_32_12$. Due to the weakness of the superstructure, only the substructure reflection lines can be observed on the X-ray powder spectra (Table II). The $Ta_4P_4S_{29}$ tetragonal parameters were refined from a Guinier powder spectrum (Guinier Nonius FR 552, $\lambda CuK\alpha_1 = 1.54051$ Å, Si as standard) (Table II), by a least-squares technique, taking into account the 87 first reflections. Because of the existence of composition close $TaPS_6$ (*14*), this compound was also prepared as standard for $Ta_4P_4S_{29}$ microprobe analysis. In addition, to check the purity of both phases, the powder spectrum of $TaPS_6$ was also recorded, and its parameters refined from the 60 first reflexions as described above (Table III). Within experimental error, the calculated $TaPS_6$ parameters are identical to those published by Fiechter *et al.* (*14*). Powder spectra tables are reported for both $TaPS_6$ and $Ta_4P_4S_{29}$ along with the observed and calculated interplanar distances of reflection planes and with intensities calculated from the Lazy Pulverix program (*15*) for a Guinier–Hägg camera with a quartz crystal monochromator.

The crystal selected for intensity recording on the Nonius CAD4 diffractometer was a small elongated parallelepiped block rotated along the c axis (Table I). Intensities were corrected for absorption, using as for the data reduction, structure solution and refinement, the SDP-PLUS program chain (1982 version) of Enraf-Nonius, written by Frenz (*16*) (Table I).

3. Structure Refinement

A structural determination was first conducted with only the substructure data in $P4_22_12$ space group. Peaks in the Patterson map revealed the full occupancy of the eightfold equipoint (b) by one Ta, one phosphorus and six sulfur atoms, which corresponds to the formula $TaPS_6$. From these first positions, a refinement, conducted with anisotropic factors, leads to a value of $R = 0.058$, with 2158 reflections and 101 variables.

At that point, a drawing showed the structure to be representable by a basic tunnel framework (Fig. 1), while a Fourier difference map indicated the remaining sulfur to be distributed in the tunnels.

Taking into account the superstructure (177 extra reflections), the refinement was then resumed in the $P4_32_12$ space group, all the atoms being found in eightfold equipoints (b), except for one sulfur atom (SC) in the fourfold equipoint (a), with full occupancy of all the sites. The sulfur atoms located in the tunnels of the structure were

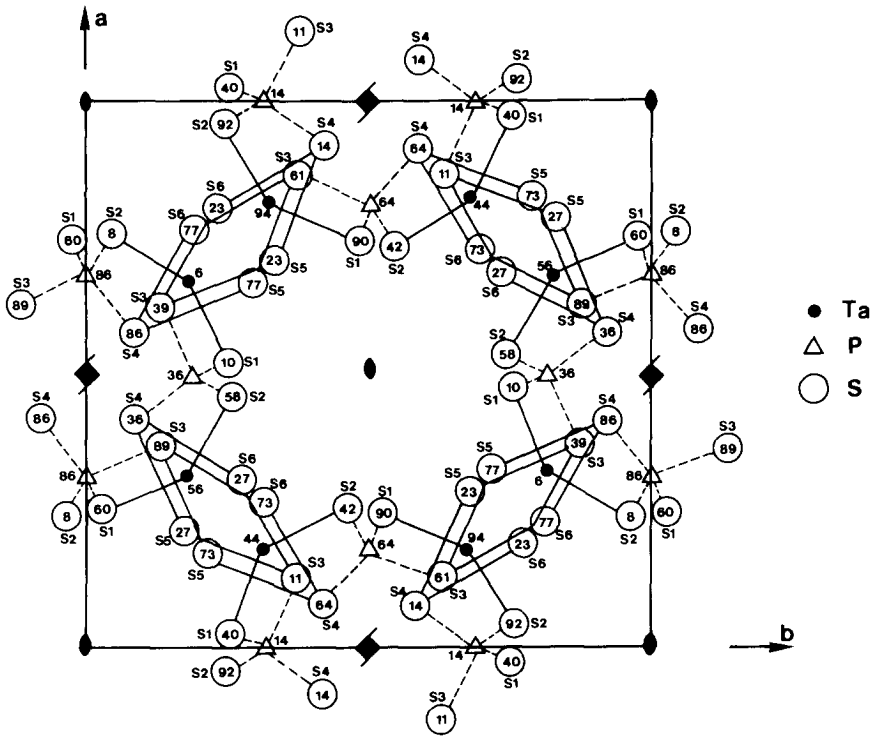

FIG. 1. Projection along the c axis, and in a subcell, of the basic tunnel structure (BTS) of $Ta_4P_4S_{29}$ obtained from a first calculation in $P4_22_12$ space group. Numbers represent the heights ($\times 100$) of the atoms.

found to form a right-handed chain giving rise to the $2c$ superstructure (see Section 4). Because of the strong correlation between atoms equivalent in the $P4_22_12$ space group and related to each other by a $c/2$ glide in the supercell, their corresponding thermal anisotropic β_{ij} factors were set identical in the refinement calculations. The reliability factor being calculated under these conditions was $R = 0.033$ with 2335 reflexions and 146 independent variables. The Fourier difference map then calculated was featureless (Table I).

Calculations were also performed in $P4_12_12$, as this group was allowed by the extinction conditions. Considering the important part to the diffraction power of the $TaPS_6$ framework, and since the atoms of the substructure can be related satisfactorily to each other in either space group, such a possibility could not be entirely ruled out, in spite of the very satisfactory results obtained in $P4_32_12$ group. The refinement conducted in $P4_12_12$ with the same conditions as described above led to a higher reliability value ($R = 0.040$), with negative anisotropic thermal factors for some sulfur atoms. This eliminated $P4_12_12$ as a possible space group for $Ta_4P_4S_{29}$.

In Tables IV and V are collected the final positional and thermal atomic parameters of the structure (structure factor tables to be sent upon request).

4. Structural Results and Discussion

Tables VI, VII, and VIII specify the main distances and angles of $Ta_4P_4S_{29}$ structure.

TABLE IV

$Ta_4P_4S_{29}$ Positional Parameters and Their Estimated Standard Deviations

Atom	X	Y	Z	B (Å²)
TA	0.18008(4)	0.67055(4)	0.77902(4)	0.667(8)
TA′	0.18188(4)	0.66914(4)	0.28050(5)	0.7
S1	0.2544(3)	0.0210(3)	0.9529(3)	1.06(3)
S1′	0.2517(3)	0.0203(3)	0.4498(3)	1.1
S2	0.2468(3)	0.4628(3)	0.0401(3)	1.13(3)
S2′	0.2547(3)	0.4593(3)	0.5438(3)	1.1
S3	0.1273(3)	0.3667(3)	0.1957(3)	1.09(3)
S3′	0.1266(3)	0.3643(3)	0.6967(3)	1.1
S4	0.4180(3)	0.0847(3)	0.0719(3)	1.00(3)
S4′	0.4192(3)	0.0858(3)	0.5684(3)	1.0
S5	0.2142(3)	0.1762(3)	0.1138(3)	1.12(3)
S5′	0.2149(3)	0.1742(3)	0.6128(3)	1.1
S6	0.3050(3)	0.2711(3)	0.1178(3)	1.07(3)
S6′	0.3034(3)	0.2700(3)	0.6178(3)	1.1
P	0.1837(3)	0.5067(3)	0.9290(3)	0.89(3)
P′	0.1849(3)	0.5071(3)	0.4295(3)	0.9
SA	0.5557(4)	0.5327(4)	0.6537(4)	2.3(1)
SB	0.4460(4)	0.5137(4)	0.4482(4)	2.3(1)
SC	0.0451(4)	0.045	0.000	2.51(9)

Note. Anisotropically refined atoms are given in the form of the isotropic equivalent thermal parameter defined as $4/3 * [a^2 \cdot B(1,1) + b^2 \cdot B(2,2) + c^2 * B(3,3) + ab(\cos\gamma) * B(1,2) + ac(\cos\beta) * B(1,3) + bc(\cos\alpha) * B(2,3)]$.

As in most of the *M*–P–S phases of VD elements (see, for example (*8–14*)), the typical bicapped biprismatic $[Ta_2S_{12}]$ (Fig. 2) and tetrahedral $[PS_4]$ constituent units are also encountered in this compound.

In the capped prisms, the Ta atoms have eight S neighbors with distances ranging

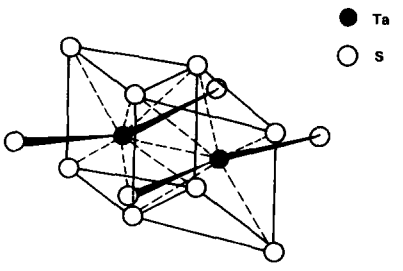

FIG. 2. Perspective drawing of the constitutive $[Ta_2S_{12}]$ bicapped biprismatic unit of the BTS

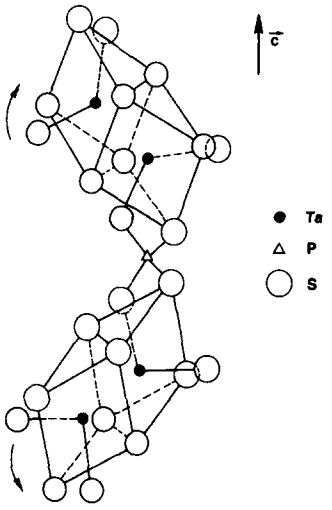

FIG. 3. $[Ta_2S_{12}]$ groups linked through a $[PS_4]$ tetrahedron. The arrows indicate the direction of tilting of the biprisms as compared to $TaPS_6$ similar arrangement.

from 2.446 to 2.610 Å, for an average of 2.539 Å. The Ta atoms occur in pairs, with d_{Ta-Ta} = 3.384 Å, as do four sulfur atoms (S5–S5, S6–S6) constituting the rectangular sulfur face common to both $[TaS_8]$ prisms (average d_{S-S} =2.039 Å). The $[PS_4]$ tetrahedra (average d_{P-S} = 2.044 Å) are formed with two sulfur-sharing $[Ta_2S_{12}]$ biprisms, as shown on Fig. 3. Such linking spreads over the structure to form a three-dimensional network constituting a basic tunnel structure (called BTS below) corresponding to the formula $TaPS_6$ (Fig. 1). Since a $TaPS_6$ compound has already been reported (*14*), it was of interest to compare it to the BTS of $Ta_4P_4S_{29}$, before examining the sulfur atoms which are inserted in the tunnels of this compound and which are responsible for the composition difference between both phases. This comparison appears quite justified, since, as will be seen below, the inserted sulfur chain is loosely bonded to the BTS and can be assumed to interfere only very weakly with it.

Although $TaPS_6$ crystallizes in a tetragonal-centered cell ($I4_1/acd$), its structure

TABLE V

REFINED TEMPERATURE FACTOR EXPRESSIONS—BETA'S

Name	$B(1,1)$	$B(2,2)$	$B(3,3)$	$B(1,2)$	$B(1,3)$	$B(2,3)$
TA	0.00067(2)	0.00070(2)	0.00090(2)	−0.00022(3)	−0.00008(4)	0.00011(4)
TA′	$B(1,1)$	$B(2,2)$	$B(3,3)$	$B(1,2)$	$B(1,3)$	$B(2,3)$
S1	0.00125(7)	0.00105(7)	0.0013(1)	−0.0001(1)	0.0004(1)	−0.0002(1)
S1′	$B(1,1)$	$B(2,2)$	$B(3,3)$	$B(1,2)$	$B(1,3)$	$B(2,3)$
S2	0.00125(7)	0.00109(7)	0.0015(1)	−0.0005(1)	−0.0008(2)	0.0006(2)
S2′	$B(1,1)$	$B(2,2)$	$B(3,3)$	$B(1,2)$	$B(1,3)$	$B(2,3)$
S3	0.00097(7)	0.00145(7)	0.00122(8)	−0.0004(1)	0.0002(1)	−0.0007(1)
S3′	$B(1,1)$	$B(2,2)$	$B(3,3)$	$B(1,2)$	$B(1,3)$	$B(2,3)$
S4	0.00091(7)	0.00097(7)	0.00160(8)	0.0000(1)	−0.0005(1)	0.0002(1)
S4′	$B(1,1)$	$B(2,2)$	$B(3,3)$	$B(1,2)$	$B(1,3)$	$B(2,3)$
S5	0.00123(7)	0.00116(7)	0.00140(9)	0.0004(1)	0.0004(1)	0.0003(2)
S5′	$B(1,1)$	$B(2,2)$	$B(3,3)$	$B(1,2)$	$B(1,3)$	$B(2,3)$
S6	0.00117(7)	0.00119(7)	0.00122(9)	0.0005(1)	−0.0002(1)	−0.0002(1)
S6′	$B(1,1)$	$B(2,2)$	$B(3,3)$	$B(1,2)$	$B(1,3)$	$B(2,3)$
P	0.00102(7)	0.00084(7)	0.00116(9)	−0.0001(1)	0.0001(2)	0.0003(1)
P′	$B(1,1)$	$B(2,2)$	$B(3,3)$	$B(1,2)$	$B(1,3)$	$B(2,3)$
SA	0.0022(2)	0.0032(2)	0.0023(2)	−0.0016(4)	0.0008(4)	−0.0005(4)
SB	0.0019(2)	0.0034(2)	0.0026(3)	0.0002(4)	−0.0003(4)	0.0004(4)
SC	0.0030(2)	$B(1,1)$	0.0024(3)	−0.0012(6)	0.0016(4)	$-B(1,3)$

Note. The form of the anisotropic thermal parameter is $\exp[-(B(1,1) * H^2 + B(2,2) * K^2 + B(3,3) * L^2 + B(1,2) * HK + B(1,3) * HL + B(2,3) * KL)]$.

TABLE VI

MAIN INTERATOMIC DISTANCES (IN Å) IN $Ta_4P_4S_{29}$ (ESD IN BRACKETS)

(a) $[Ta_2S_{12}]$ biprismatic bicapped groups

Ta–Ta : 3.383(1)	Ta′–Ta′ : 3.385(1)
–S1 : 2.555(3)	–S1′ : 2.553(3)
–S2 : 2.603(4)	–S2′ : 2.577(4)
–S3 : 2.482(4)	–S3′ : 2.470(5)
–S4 : 2.453(4)	–S4′ : 2.446(4)
–S5 : 2.610(4), 2.553(3)	–S5′ : 2.605(3), 2.533(3)
–S6 : 2.535(4), 2.554(4)	–S6′ : 2.520(4), 2.573(4)
Average d_{Ta-S} = 2,539	
S6–S5 : 2.047(5)	
S6′–S5′ : 2.032(5)	Average d_{S-S} : 2.039

(b) $[PS_4]$ tetrahedral groups

P–S1 : 2.054(5)	P′–S1′ : 2.033(5)
P–S2 : 2.016(5)	P′–S2′ : 2.043(5)
P–S3 : 2.048(5)	P′–S3′ : 2.026(5)
P–S4 : 2.069(6)	P′–S4′ : 2.063(6)
	Average d_{P-S} = 2.044

(c) Polymeric $[S_{10}]_\infty$ chain

SA–SB : 2.045(3)(×4)	
SA–SC : 2.057(3)(×4)	
SB–SB : 2.057(4)(×2)	Average d_{S-S} : 2.052

features very much resembles that of the BTS. It is made up of the same $[Ta_2S_{12}]$ and $[PS_4]$ units linked in the same way, with the difference that the $[Ta_2S_{12}]$ biprisms that have their triangular faces parallel to the C face in $TaPS_6$, are tilted relative to the c axis in the BTS (see Fig. 3).

This explains the differences in parameters between both cells, with the c parameter longer and the a parameter smaller in the former phase (c = 13.652 Å and a = 15.571 Å) than in the latter one (c = 13.143 Å and a = 15.849 Å).

The geometric differences in the structures leave the interatomic distances very similar to each other, with the average distances in $TaPS_6$: d_{Ta-Ta} = 3.365 Å, d_{Ta-S} = 2.536 Å, d_{P-S} = 2.033 Å, and d_{S-S} = 2.048 Å.

Taking into account the two types of anions of the structures (S_2^{-II} and S^{-II}) and

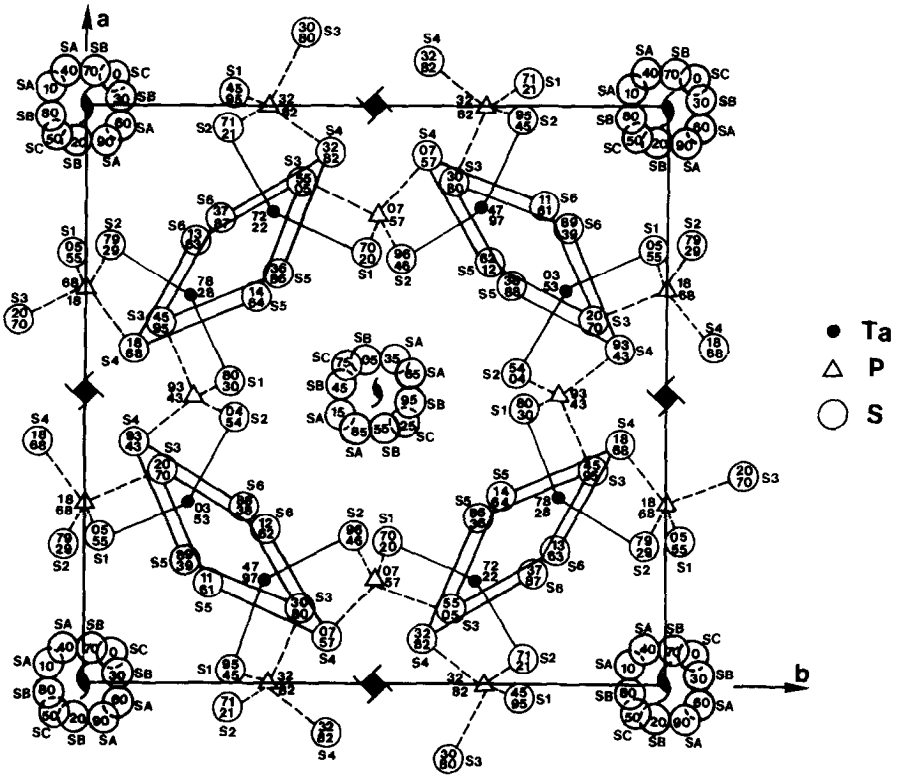

FIG. 4. $Ta_4P_4S_{29}$ structure projection along the c axis. Only a few symmetry elements have been represented. Numbers represent the heights (×100) of the atoms.

assuming an oxidation state of five for the tetrahedral phosphorus, both systems can be represented by $Ta^{V}P^{V}(S_2^{-II})(S^{-II})_4$. From this formula, and because the cation pairs are far apart, a diamagnetic susceptibility can be inferred; this has been verified for $TaPS_6$ which has a diamagnetic molar susceptibility of -109×10^{-6} emu at room temperature.

The BTS structure found in a first calculation step of $Ta_4P_4S_{29}$ corresponds, in the elementary supercell, to the composition $16(TaPS_6)$. The remaining 20 sulfur atoms are located in the two empty tunnels of the BTS around the 2_1 axis of the structure. They form two $(S_{10})_\infty$ chains running along the c axis and are repeated every two length of the subcell (Fig. 4). These sulfur helices are found to be right-handed. The average bond distance between sulfur and the average S–S–S angle are respectively equal to 2.052 Å and 105.75°.

Figures 5 and 6 show the polymeric sulfur chains seen in perspective along the c axis and in projection, at the origin, on the (**a,b**) plane.

These results are in agreement with the bond length and S–S–S angle recorded in pressure-induced fibrous sulfur (*17*) for which a S–S bond length of 2.07 Å and a S–S–S angle of 106° are reported.

As can be deduced from sulfur–sulfur distances (Table VIII), no bonding other than the van der Waals type exists between the $(S_{10})_\infty$ helices and the BTS surrounding sulfur atoms, since the shortest S–S distance is found equal to 3.306 Å. As has been shown elsewhere (*8–13*) in the *M*–P–

TABLE VII

MAIN ANGLES (IN DEGREES) IN $Ta_4P_4S_{29}$ (ESD IN BRACKETS)

(a) $[Ta_2S_{12}]$ bicapped biprims

triangular faces

S5–S4–S6 : 34.10(10)	S6–S3–S5 : 35.2(1)
S4–S5–S6 : 71.0(2)	S3–S5–S6 : 69.0(2)
S4–S6–S5 : 74.9(2)	S5–S6–S3 : 75.9(2)
S5′–S4′–S6′ : 33.9(1)	S6′–S3′–S5′ : 34.9(1)
S4′–S5′–S6′ : 71.3(2)	S3′–S5′–S6′ : 68.3(2)
S4′–S6′–S5′ : 74.8(2)	S5′–S6′–S3′ : 76.8(2)

Rectangular faces

S4–S6–S6 : 92.3(2)	S4′–S6′–S6′ : 91.3(2)
S6–S6–S3 : 96.2(2)	S6′–S6′–S3′ : 96.7(2)
S6–S3–S4 : 86.1(1)	S6′–S3′–S4′ : 85.9(1)
S3–S4–S6 : 85.4(1)	S3′–S4′–S6′ : 85.9(1)
S4–S3–S5 : 86.3(1)	S4′–S3′–S5′ : 86.7(1)
S3–S5–S5 : 94.7(2)	S3′–S5′–S5′ : 94.2(2)
S5–S5–S4 : 94.6(2)	S5′–S5′–S4′ : 95.2(2)
S5–S4–S3 : 84.0(1)	S5′–S4′–S3′ : 83.9(1)
S6–S5–S5 : 91.1(2)	S6′–S5′–S5′ : 91.2(2)
S5–S6–S6 : 88.8(2)	S5′–S6′–S6′ : 88.6(2)

(b) $[PS_4]$ tetraedra

S1–P–S2 : 115.6(2)	S1′–P′–S2′ : 116.2(2)
S1–P–S3 : 100.2(2)	S1′–P′–S3′ : 101.1(2)
S1–P–S4 : 114.6(2)	S1′–P′–S4′ : 116.2(2)
S2–P–S3 : 116.3(3)	S2′–P′–S3′ : 116.6(3)
S2–P–S4 : 101.5(2)	S2′–P′–S4′ : 98.4(2)
S3–P–S4 : 109.1(2)	S3′–P′–S4′ : 109.0(2)

SA–SB–SB : 107.02(13)(×4)
SB–SA–SC : 104.66(12)(×4)
SA–SC–SA : 105.38(15)(×2)

Average α_{S-S-S} : 105.75°

TABLE VIII

SHORTEST INTERATOMIC DISTANCES (IN Å) BETWEEN THE SULFUR ATOMS OF THE $(S_{10})_\infty$ HELIX AND NEIGHBOR SULFURS OF THE $(TaPS_6)$ FRAMEWORK (ESD) IN BRACKETS)

S1–SA : 3.715(4)	S2–SA : 3.306(4)	S5′–SB : 3.830(4)
S1–SC : 3.344(4)	S2–SB : 3.849(4)	S6 –SA : 3.778(4)
S1′–SA : 3.741(4)	S2′–SB : 3.361(4)	
S1′–SB : 3.683(4)	S5–SC : 3.675(4)	

S phases, the S–S bond is expected to remain below 3.0 Å; this is a much shorter distance than that found here.

Only van der Waals forces thus hold the polymeric sulfur in the structure; it is thought to be the first time that such chalcogen infinite helices are reported as trapped in a tridimensional network. Since fibrous sulfur (*17*) present alternatively left-handed and right-handed sulfur helices, the question may be raised as why, in $Ta_4P_4S_{29}$, a single type of polymeric sulfur is found. It is possible that, under the influence of temperature, for example, a reorientation of the helix from right- to left-handed may take place, leading either to a complete transformation, or to a partial one in an ordered or random array.

In Table IV are found the equivalent thermal factors; it should be pointed out that the *B* values of the chain sulfur atoms are considerably higher than those of the BTS ($B \simeq 2.4$ Å^2 as compared to $B \simeq 1.1$

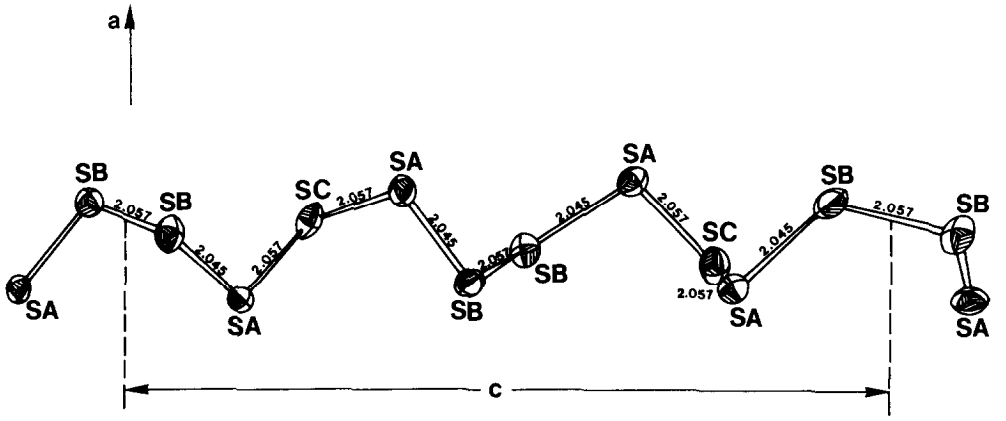

FIG. 5. Perspective drawing, along the *c* axis, of the $[S_{10}]_\infty$ helix encountered in $Ta_4P_4S_{29}$. (Drawing by ORTEP program). Sulfur–sulfur distances in Ångstroms.

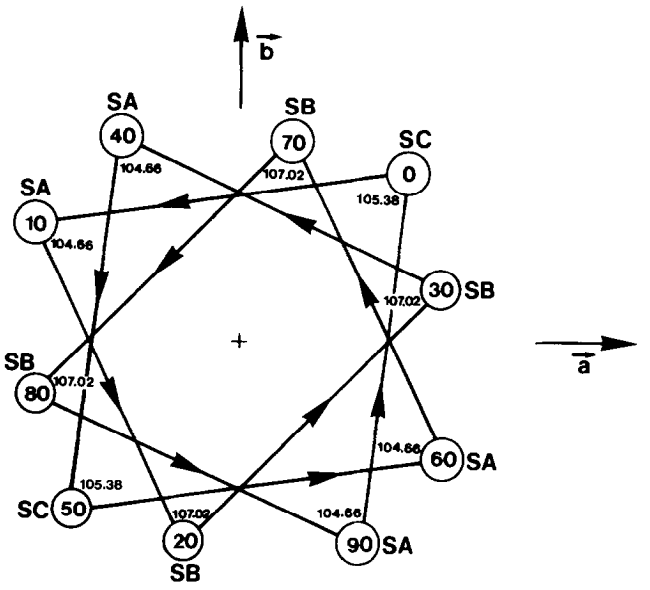

FIG. 6. Projection along the c axis of the $[S_{10}]_\infty$ helix. Angles in degrees.

Å^2). Although this is not an uncommon difference among the M–P–S phases (see, for example (*8–9*)), some explanation for it can be put forward in $Ta_4P_4S_{29}$ case. Because of the weak bonding between the BTS and $(S_{10})_\infty$ chains, a greater freedom of movement can for example be envisioned for the helical sulfur atoms, since the BTS presents a rigid covalent tridimensional arrangement. It is also possible to imagine some degree of discommensuration between the BTS and the helices, resulting in an apparent unsharpness of the positions.

This situation can be correlated to the length of the pressure-induced fibrous sulfur with its similar $(S_{10})_\infty$ chains. The length of the periodic (S_{10}) portion of the chains is, in this phase, equal to 13.80 Å, as compared to 13.65 Å for the same (S_{10}) group in $Ta_4P_4S_{29}$. Although the pressure effect may be responsible for the difference, a discommensuration in the tantalum compound also appears to provide a possible explanation.

From the structural features given above, the formula $Ta_4P_4S_{29}$ can thus be written as $Ta_4^{V}P_4^{V}(S^{-II})_{16}(S_2^{-II})_4(S^0)_5$. This formulation implies again, and for some of the reasons put forward for $TaPS_6$, a diamagnetic molar susceptibility which is found equal to -480×10^{-6} emu/mole at room temperature.

5. Conclusion

$Ta_4P_4S_{29}$ is a new phase of the Ta–P–S system that presents a new combination between a tridimensional network and polymeric sulfur only bonded to each other by weak van der Waals forces. The tunnel framework has the composition $TaPS_6$ and is made of bicapped biprisms $[Ta_2S_{12}]$ linked to each other through $[PS_4]$ tetrahedral units. The sulfur, located in both tunnels of the basic $TaPS_6$ tridimensional array, develops along the c axis over two lengths of the subcell as right-handed helices. In some respect, this phase can thus be looked at as a kind of composite material. Because of the novel structural features of the phase, the Ta–P–S system is currently further explored.

References

1. M. C. FRIEDEL, *Bull. Soc. Chim. Fr.* **11,** 1057 (1894).
2. H. HAHN AND W. KINGEN, *Naturwissenschaften* **52,** 494 (1965).
3. W. KLINGEN, G. EULENBERGER, AND H. HAHN, *Naturwissenschaften* **55,** 229 (1968).
4. W. KLINGEN, Ph.D. Höhenheim, W.G. (1969).
5. W. KLINGEN, AND P. WILD, *Mater. Res. Bull.* **5,** 519 (1970).
6. W. KLINGEN, R. OTT, AND H. HAHN, *Z. Anorg. Allg. Chem.* **396,** 271 (1973).
7. R. BREC, G. OUVRARD, R. FREOUR, J. ROUXEL, AND J. L. SOUBEYROUX, *Mater. Res. Bull.* **18,** 689 (1983).
8. R. BREC, G. OUVRARD, M. EVAIN, P. GRENOUILLEAU, AND J. ROUXEL, *J. Solid State Chem.* **47,** 174 (1983).
9. M. EVAIN, R. BREC, G. OUVRARD, AND J. ROUXEL, *J. Solid State Chem.* **56,** 12 (1985).
10. R. BREC, P. GRENOUILLEAU, M. EVAIN, AND J. ROUXEL, *Rev. Chim. Min.* **20,** 295 (1983).
11. R. BREC, M. EVAIN, P. GRENOUILLEAU, AND J. ROUXEL, *Rev. Chim. Min.* **20,** 283 (1983).
12. P. GRENOUILLEAU, R. BREC, M. EVAIN, AND J. ROUXEL, *Rev. Chim. Min.* **20,** 628 (1983).
13. M. EVAIN, R. BREC, G. OUVRARD, AND J. ROUXEL, *Mater. Res. Bull.* **19,** 41 (1984).
14. S. FIECHTER, W. F. KUHS, AND R. NITSCHE, *Acta Crystallogr. Sect. B* **36,** 2217 (1980).
15. R. YVON, W. JEITSCHKO, AND E. PARTHE, *J. Appl. Crystallogr.* **10,** 73 (1977).
16. B. FRENZ, "Enraf-Nonius, Structure Determination Package," Delft, Univ. Press (1982).
17. M. D. LIND AND S. GELLER, *J. Chem. Phys.* **51,** 1, 348 (1959).